Journal of the American College of Cardiology
© 1999 by the American College of Cardiology
Published by Elsevier Science Inc.

Vol. 35, No. 1, 2000
ISSN 0735-1097/00/$20.00
PII S0735-1097(99)00499-4

Regional Myocardial Blood Flow Reserve Impairment and Metabolic Changes Suggesting Myocardial Ischemia in Patients With Idiopathic Dilated Cardiomyopathy

Ad F. M. van den Heuvel, MD, Dirk J. van Veldhuisen, MD, PHD, FACC, Ernst E. van der Wall, MD, PHD, FACC,* Paul K. Blanksma, MD, PHD, Hans-Marc J. Siebelink, MD, Willem M. Vaalburg, PHD,† Wiek H. van Gilst, PHD, Harry J. G. M. Crijns, MD, PHD

Groningen and Leiden, The Netherlands

OBJECTIVES We performed positron emission tomography (PET) to evaluate myocardial ischemia in patients with idiopathic dilated cardiomyopathy (IDC).

BACKGROUND Patients with IDC have anatomically normal coronary arteries, and it has been assumed that myocardial ischemia does not occur.

METHODS We studied 22 patients with IDC and 22 control subjects using PET with nitrogen-13 ammonia to measure myocardial blood flow (MBF) at rest and during dipyridamole-induced hyperemia. To investigate glucose metabolism, fluorine-18 deoxyglucose (^{18}FDG) was used. For imaging of oxygen consumption, carbon-11 acetate clearance rate constants (k_{mono}) were assessed at rest and during submaximal dobutamine infusion (20 μg/kg body weight per min).

RESULTS Global MBF reserve (dipyridamole-induced) was impaired in patients with IDC versus control subjects (1.7 ± 0.21 vs. 2.7 ± 0.10, $p < 0.05$). In patients with IDC, MBF reserve correlated with left ventricular (LV) systolic wall stress ($r = -0.61$, $p = 0.01$). Furthermore, in 16 of 22 patients with IDC (derived by dipyridamole perfusion) mismatch (decreased flow/increased ^{18}FDG uptake) was observed in 17 ± 8% of the myocardium. The extent of mismatch correlated with LV systolic wall stress ($r = 0.64$, $p = 0.02$). The MBF reserve was lower in the mismatch regions than in the normal regions (1.58 ± 0.13 vs. 1.90 ± 0.18, $p < 0.05$). During dobutamine infusion k_{mono} was higher in the mismatch regions than in the normal regions (0.104 ± 0.017 vs. 0.087 ± 0.016 min^{-1}, $p < 0.05$). In the mismatch regions ^{18}FDG uptake correlated negatively with rest k_{mono} ($r = -0.65$, $p < 0.05$), suggesting a switch from aerobic to anaerobic metabolism.

CONCLUSIONS Patients with IDC have a decreased MBF reserve. In addition, low MBF reserve was paralleled by high LV systolic wall stress. These global observations were associated with substantial myocardial mismatch areas showing the lowest MBF reserves. In geographically identical regions an abnormal oxygen consumption pattern was seen together with a switch from aerobic to anaerobic metabolism. These data support the notion that regional myocardial ischemia plays a role in IDC. (J Am Coll Cardiol 2000;35:19–28) © 1999 by the American College of Cardiology

Idiopathic dilated cardiomyopathy (IDC) is a primary myocardial disease of unknown origin, characterized by a poorly contracting and dilated left or right ventricle (1). Idiopathic dilated cardiomyopathy leads to symptomatic congestive heart failure (CHF) in the majority of patients and carries a high morbidity and mortality rate (2). It has generally been assumed that in patients with IDC, myocardial ischemia does not play a role, because they have, by definition, anatomically normal epicardial coronary arteries. However, recent studies have shown that endothelial function is impaired in patients with IDC (3) and that myocardial perfusion abnormalities occur (4). It is unknown whether this leads to abnormal metabolism compatible with myocardial ischemia.

Dynamic positron emission tomographic (PET) imaging permits noninvasive quantitation of myocardial blood flow (MBF) and metabolism by using positron-emitting imaging tracers taken up by the myocardium (5). Myocardial blood

From the Department of Cardiology, University Hospital Groningen, Groningen; *Department of Cardiology, Leiden University Medical Center, Leiden; and †National Positron Emission Tomography Center, University Hospital Groningen, Groningen, The Netherlands.

Manuscript received March 19, 1999; revised manuscript received July 27, 1999, accepted September 14, 1999.

JACC Vol. 35, No. 1, 2000
January 2000:19–28

Abbreviations and Acronyms

ACE = angiotensin-converting enzyme
CHF = congestive heart failure
CI = confidence interval
^{18}FDG = fluorine-18 deoxyglucose
IDC = idiopathic dilated cardiomyopathy
LV = left ventricular
LVEF = left ventricular ejection fraction
MBF = myocardial blood flow
NYHA = New York Heart Association
PET = positron emission tomography
$\dot{V}O_2$max = peak oxygen consumption

flow is estimated using nitrogen-13 (^{13}N)-ammonia as a perfusion tracer (6,7), both at rest and after application of vasodilating agents such as dipyridamole to assess MBF reserve. Fluorine-18 deoxyglucose (^{18}FDG) is a positron-emitting metabolic imaging tracer with higher uptake by the myocardium in the presence of chronic ischemia and low uptake in infarct-related regions. Simultaneous imaging with ^{13}N-ammonia and ^{18}FDG can demonstrate regions of mismatch, where reduced uptake of ^{13}N-ammonia but retained uptake of ^{18}FDG is indicative of viable myocardium (8). These mismatch patterns have been shown to be a good marker for identifying myocardial viability in patients with coronary artery disease (9). In addition to these tracers, carbon-11 (^{11}C)-acetate is used to quantitate myocardial oxidative metabolism. This tracer enters the mitochondria and participates as ^{11}C-acetyl-coenzyme A in the tricarboxylic acid cycle. The ^{11}C activity is released from the myocardium as [^{11}C]CO_2. Both monoexponential and biexponential clearance of ^{11}C activity from the myocardium after intravenous injection of ^{11}C-acetate (10,11) is used to estimate oxygen consumption. Quantification of the clearance kinetics of this tracer from the myocardium allows estimation of myocardial oxygen consumption. Increased cardiac work load is associated with an increase in the ^{11}C-acetate clearance rate constant (k_{mono}) (11). These characteristics make ^{11}C-acetate a useful tracer for clinical research to determine myocardial oxygen consumption.

The present study investigated whether MBF reserve impairment in patients with IDC is related to ischemic changes, thereby playing a potential role in the development or progression of the disease. We examined MBF and MBF reserve, myocardial glucose metabolism and oxygen consumption in patients with IDC using PET, and we compared these data with those of a group of age- and gender-matched normal volunteers (control subjects). Further, we investigated echocardiographic left ventricular (LV) wall stress, which is a well-known factor determining MBF.

METHODS

Study group. Patients with IDC and mild to moderate CHF were eligible for the study and were compared with a group of age- and gender-matched healthy volunteers (control subjects). All patients underwent coronary angiography, which showed normal epicardial coronary arteries. The diagnosis of IDC, on the basis of a combination of clinical variables (LV dilation, global decreased contraction patterns), was supported by endomyocardial biopsy. In all 22 patients, microscopic features included hypertrophy as well as degeneration of myocytes and varying degrees of interstitial fibrosis. At baseline, within seven days of PET, the severity of CHF was assessed by scoring functional class according to the New York Heart Association (NYHA), by measuring LV ejection fraction (LVEF) using equilibrium radionuclide ventriculography and by determining peak oxygen consumption ($\dot{V}O_2$max) on a treadmill with respiratory gas exchange measurements as previously described (12). All patients had to be clinically stable on angiotensin-converting enzyme (ACE) inhibitors, diuretics and digoxin. Other vasoactive medications, including beta-blockers, were not allowed. Patients with systemic hypertension (systolic blood pressure >150 mm Hg, diastolic blood pressure >95 mm Hg), diabetes mellitus, hypercholesterolemia (>6 mmol/liter) or any other systemic illness were excluded. Healthy control subjects were selected from our data base and matched for age and gender. All participants underwent a physical examination, electrocardiogram and laboratory analysis (total cholesterol, renal function, electrolytes, hemoglobin). All patients gave written, informed consent, and the protocol was approved by the Institutional Review Board.

Protocol for PET imaging. The PET studies were performed after patients (and control subjects) had refrained from medical therapy for five plasma half-lives and caffeinated beverages for 24 h before the studies. Patients were positioned in a 951 Siemens (ECAT) positron camera (Siemens AG, Knoxville, Tennessee), which images 31 planes simultaneously over 10.8 cm (axial field of view). Data were automatically corrected for accidental coincidence and dead time. Subjects were positioned with the help of a rectilinear scan. Photon attenuation was measured using a rectilinear external ring source filled with ^{68}Ge/^{68}Ga. Patients were constantly monitored with 12-lead electrocardiography, and blood pressure was measured automatically every 10 min and every minute during dipyridamole and dobutamine infusion. Myocardial blood flow was studied according to the methods of Schelbert et al. (6) and Bellina et al. (7), as previously described (13), using ^{13}N-ammonia as the tracer. Dynamic rest imaging was started at the time of ^{13}N-ammonia injection (370 MBq) and continued for 15 min (frames 12 × 10 s, 1 × 2 min, 1 × 4 min, 1 × 7 min). Dipyridamole stress imaging was performed by infusing dipyridamole (0.56 mg/kg body weight in 4 min). Imaging was done by injecting 370 MBq of ^{13}N-ammonia 6 min after the start of dipyridamole infusion and continued for 15 min (frames 12 × 10 s, 1 × 2 min, 1 × 4 min, 1 × 7 min). After this, myocardial glucose uptake was

studied with ^{18}FDG, using the methods of Choi et al. (14). To stimulate myocardial glucose uptake, patients were given 75 g of glucose orally before the scanning procedure. The FDG imaging was done 5 min after injecting 185 MBq of ^{18}FDG and continued for 35 min (frames 8 × 15 s, 4 × 30 s, 1 × 1 min, 1 × 5 min, 1 × 10 min, 1 × 15 min). On a separate day, within 1 week of ^{13}N-ammonia and ^{18}FDG PET imaging, oxidative metabolism was determined by measuring the ^{11}C-acetate clearance rate constants (k_{mono}) (10). Data correction, positioning and photon attenuation were done as described earlier. Carbon-11–acetate rest imaging was performed by injecting 370 MBq of ^{11}C-acetate, and imaging was done for 35 min (frames 12 × 10 s, 8 × 1 min, 5 × 2 min, 5 × 3 min). Then dobutamine infusion was started at 5 μg/kg per min. The dose was increased with 5 μg/kg per min every 2 min until 20 μg/kg per min maximum was achieved. Infusion was continued at 20 μg/kg per min for the rest of the study to maintain a constant rate–pressure product, and 11 min after the start of dobutamine infusion 370 MBq of ^{11}C-acetate was injected. Imaging continued for 20 min (frames 12 × 10 s, 8 × 1 min, 5 × 2 min).

Analysis of PET data. The data from the dipyridamole ^{13}N-ammonia and ^{18}FDG and the dobutamine ^{11}C-acetate studies were corrected for remaining activity by subtracting the last frame of the preceding study (13). After this subtraction procedure, data for each study were reoriented to 10 short-axis images using a manually drawn long axis in the left ventricle. The myocardium in the 10 slices was divided into 48 segments (7.5° each). Using the maximal activity, time-activity curves were established in all segments of all slices (15). The blood pool was defined in three slices near the base, the average of which was used to calculate a single blood-pool time-activity curve. For each of the 480 segments MBF was calculated using a curve fit over 120 s. As this apparent flow-time curve is noisy, an exponential fit of the total data set was calculated, and the flow was measured at 90 s. To compensate for flow-mediated extraction, a correction was applied as given by Shah et al. (16): $E = E_0 \cdot (1 - 0.607 \cdot e^{-1.25/flow})$. For calculation of glucose consumption, myocardial and blood-pool time-activity curves were used to perform Patlak analysis (17). This technique is used in general models in which the tracer is irreversibly trapped in a system. It was proposed and described by Patlak and Blasberg (17). Data obtained from 5-min postinjection were used to calculate the slope of the Patlak curve. This graphic approach permits the calculation of regional ^{18}FDG uptake by giving a direct estimate of the slope of the linear relationship on the plot. To assess oxidative metabolism, ^{11}C-acetate clearance rate constants (K_{mono}) were obtained from the decay-corrected ^{11}C-acetate time-activity curves by least-square monoexponential curve fitting, as previously described (10). For each individual segment myocardial perfusion, glucose metabolism and oxidative metabolism were calculated. From these data a parametric polar map for each modality was constructed—for the ^{13}N-ammonia perfusion studies using the aforementioned perfusion model (15), for the ^{18}FDG studies using Patlak analysis (17) and for ^{11}C-acetate using the clearance rate constants (k_{mono}) (10). From the polar maps of the control case and after provocation with dipyridamole and dobutamine, ratio polar maps were constructed for MBF and oxidative metabolism, respectively. From the normal volunteers' data, we defined 95% confidence intervals (CIs) of the normal values for each imaging modality for each of the 480 segments (from mean −2 × SD to mean +2 × SD) (13,17). Patient data were then compared with these intervals in each imaging modality, resulting in a 95% confidence map for each imaging modality. This comparison shows which myocardial segment is within, above or below the corresponding 95% CI. In this way the percent myocardium above and below the 95% CI could be calculated. Global measurements are presented as the mean of the 480 segments. The parametric polar map, displaying 480 segments (13), obviates tedious selection of regions of interest. This enables selection of the three different kinds of regions (normal, match and mismatch) and to calculate flow reserve (^{13}N-ammonia), glucose metabolism (^{18}FDG uptake) and oxygen consumption (^{11}C-acetate clearance rates) in these three separate regions of interest.

Definition of blood flow (^{13}N-ammonia) vs. ^{18}FDG (mismatch and match). Vanoverschelde et al. (18) showed that dipyridamole-derived myocardial perfusion correlates better with the extent of wall motion abnormalities in hibernating myocardium, as compared with rest perfusion. Therefore, to calculate mismatch (and match) we used the dipyridamole-derived blood flow. To quantify mismatch, the parametric ^{18}FDG uptake polar map and hyperemic blood flow polar map were normalized to their mean values. A difference polar map was constructed by subtracting the normalized hyperemic MBF polar map from the normalized ^{18}FDG polar map. The percent myocardium above the 95% CI of a normal data base was calculated (Fig. 1). The results are expressed as percent total myocardium. Similarly, quantitation of match areas was determined from a product polar map by multiplying the normalized ^{18}FDG and the normalized dipyridamole-induced perfusion and by calculating the percent myocardium below the 95% CI.

Measurement of LV wall stress. Left ventricular wall stress was measured using echocardiography (19). In short, echocardiograms were recorded by a single operator, using a 2.5-MHz probe (Sonotron/Vingmed sound, Zoetermeer, The Netherlands); noninvasive blood pressure was measured simultaneously by the cuff manometer. Left ventricular internal diameter and wall thickness were obtained from M-mode tracings in the plane of the mitral valve during two-dimensional echocardiography. Left ventricular systolic wall stress was determined by the equation: $\sigma = (0.334\ P\ [LVID])/(PWT\ [1 + PWT/LVID])$, where P is the mean of duplicate cuff arterial systolic pressure; LVID is

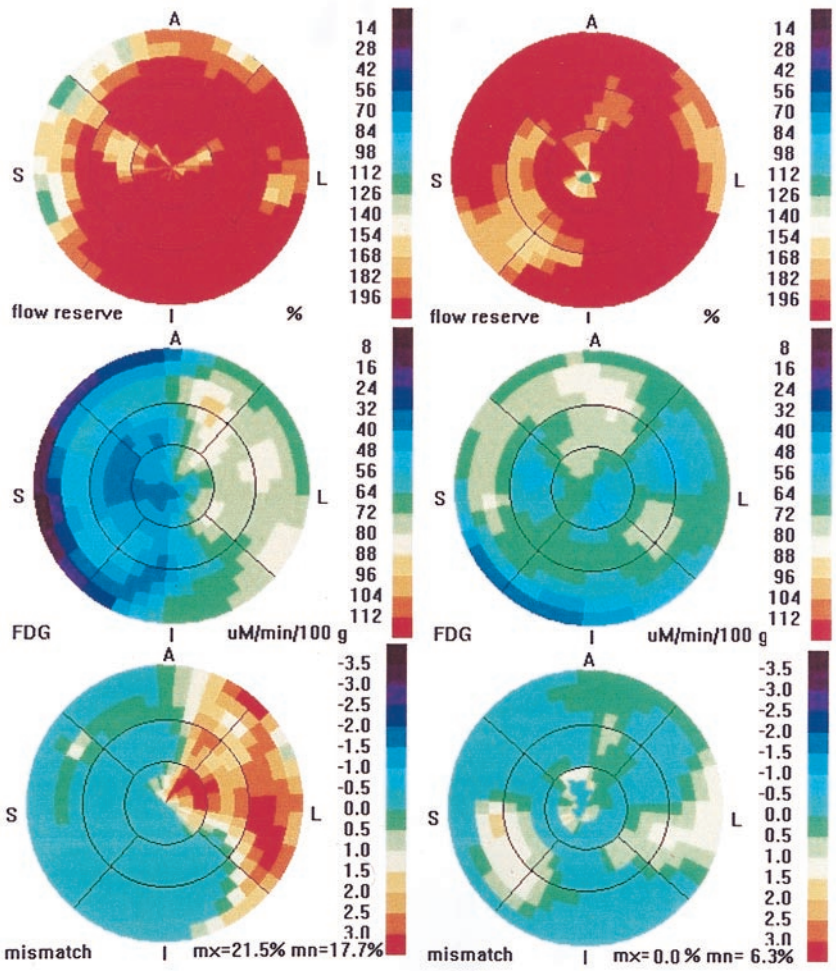

Figure 1. Example of PET polar maps. In healthy volunteers (three polar maps at right) MBF reserve (**top polar map**; 280% = ratio 2.8) and ^{18}FDG uptake (**middle polar map**; 51 μmol/min per 100 g) are more or less homogeneously distributed throughout the left ventricle. The PET polar maps in a patient with IDC (three polar maps at left) show confluent regions with mismatch **(bottom polar map)** (i.e., impaired flow reserve [top polar map; mean 210% = ratio 2.1]) paralleled by increased ^{18}FDG uptake (mean 60 μmol/min per 100 g). Flow reserve units are percent hyperemic blood flow related to rest blood flow. Mismatch units are presented as standard deviations of a normal data base. A = anterior; L = lateral; I = inferior; S = septal.

the LV systolic (smallest) internal diameter; and PWT is the systolic posterior wall thickness at the time of the smallest LVID. Data were analyzed as the mean of three to five cardiac cycles. For LV end-diastolic wall stress, P was the LV end-diastolic pressure obtained during angiography, which was performed within one day from the echocardiogram and ^{13}N-ammonia PET imaging, without changes in medication during the period between the three investigations; LVID was the LV diastolic (largest) internal diameter; and PWT was the diastolic posterior wall thickness at the time of the largest LVID. Normal systolic wall stress in our echocardiography laboratory is $106 \pm 11 \times 10^3$ dynes/cm^2; normal diastolic wall stress is $7.3 \pm 3 \times 10^3$ dynes/cm^2.

Statistical analysis. Global data are presented as the mean of 480 segments of the polar map. Data of three regions are presented, which are the mean of the regions with a normal, mismatch or match pattern. Values are given as the mean value ± SD. Group differences of perfusion dynamics were obtained using a Wilcoxon two-sample test on the deltas from baseline and during dipyridamole and dobutamine. The data of the three different regions (normal, mismatch and match) were compared by two-way analysis of variance with a Bonferroni correction. The Spearman rank-order correlation coefficient was used to investigate the associations between study variables. Differences with a p value <0.05 were considered statistically significant. Statistical analysis was performed using SAS statistical software, version 6.08. Myocardial blood flow was given in milliliters per minute/100 g, and glucose utilization in micromoles per minute/100 g. A flow-metabolism (^{13}NH3/^{18}FDG) mismatch pattern was represented as percent total myocardium. Oxidative metabolism (^{11}C-acetate clearance) was given as the rate constant (k_{mono}) per minute.

Table 1. Patient Data

Patient No.	Age (years)	Gender	NYHA Class	LVEF (%)	$\dot{V}O_2$max (ml/kg per min)	LVEDP (mm Hg)	LVSP (mm Hg)	LVEDD (mm)
1	45	F	III	53	19.9	18	100	72
2	35	M	II	23	14.2	25	110	76
3	34	M	III	16	23.9	12	108	75
4	55	F	II	18	27.2	8	120	50
5	27	M	II	27	16.4	10	100	55
6	35	F	II	53	25.9	24	110	69
7	36	F	II	24	18.9	12	100	59
8	45	F	III	40	22.6	30	110	61
9	54	M	III	29	17.2	18	100	55
10	42	M	II	29	17.2	8	100	66
11	19	M	II	27	27.5	12	120	53
12	55	M	III	51	23.9	32	110	54
13	40	M	II	18	15.9	5	115	62
14	72	F	II	21	25.3	15	100	64
15	32	M	III	32	14.0	20	115	73
16	75	M	II	16	20.7	20	110	58
17	71	M	III	31	13.1	5	100	85
18	62	F	III	15	18.9	25	105	60
19	32	M	III	34	17.8	15	100	57
20	56	M	III	33	33.2	20	110	66
21	50	M	III	20	19.5	20	110	62
22	36	M	II	23	16.1	12	110	57
mean ± SD	46 ± 15			29 ± 12	20.4 ± 5.2	17 ± 7	107 ± 7	63 ± 9

F = female; LVEDD = left ventricular end-diastolic diameter; LVEDP = left ventricular end-diastolic pressure; LVEF = left ventricular ejection fraction; LVSP = left ventricular systolic pressure; M = male; NYHA = New York Heart Association functional class for heart failure; $\dot{V}O_2$max = peak oxygen consumption.

RESULTS

Twenty-two patients with IDC and mild to moderate CHF were studied (Table 1). Total cholesterol was 5.2 ± 0.4 mmol/liter and the rest plasma norepinephrine concentration was 617 ± 20 pg/ml (normal range 100 to 500 pg/ml). The patients with IDC were compared with 22 age- and gender-matched healthy control subjects (14 men, age 44 ± 14 years, total cholesterol 5.3 ± 0.30 mmol/liter). All patients were taking an ACE inhibitor, diuretic agents and digitalis, which were discontinued 5 plasma half-lives before PET scanning. No patient was taking beta-blockers or other vasoactive drugs. The PET studies for the assessment of MBF, using ^{13}N-ammonia, and assessment of glucose utilization, using ^{18}FDG, were available in all 22 patients with IDC and control subjects. Eight patients had both match and mismatch, eight patients had only mismatch and six patients had only match. Oxygen consumption, as measured by ^{11}C-acetate clearance rates, was available in 13 patients with IDC and in all healthy control subjects. Between the two studies, patients were clinically stable and blood pressure and heart rate (rate–pressure product) were similar. The echocardiographic evaluation confirmed global LV dysfunction (global hypokinesia, i.e. impaired contraction patterns) in all patients. The LV meridional systolic wall stress was 187 ± 36 × 10^3 dynes/cm^2 (range 134 to 289 × 10^3). The LV meridional diastolic wall stress was 33 ± 18 × 10^3 dynes/cm^2 (range 6 to 64 × 10^3).

Global MBF (^{13}N-ammonia studies). At rest, global MBF was similar between patients with IDC and healthy control subjects (102 ± 21 vs. 102 ± 16 ml/min per 100 g) (Fig. 2). In contrast, after dipyridamole infusion, global MBF was significantly lower in patients with IDC as compared with control subjects (166 ± 36 vs. 280 ± 104 ml/min per 100 g, p = 0.03, delta between baseline and

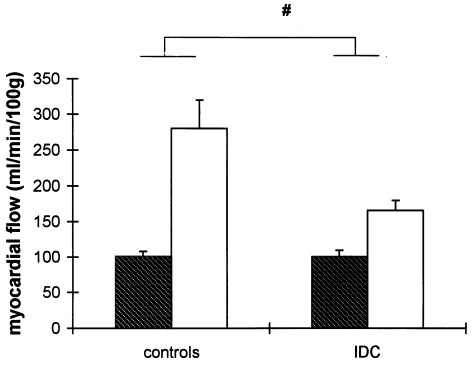

Figure 2. Global myocardial blood flow at rest **(dark hatched bars)** and after dipyridamole infusion **(open bars)** in patients with CHF and IDC and in control subjects. #p < 0.05 delta flow in healthy volunteers versus patients with IDC.

JACC Vol. 35, No. 1, 2000
January 2000:19–28

Table 2. Relations Between Hemodynamic Data and PET Data

	Rest MBF		MBF Reserve*		Acetate Clearance (Rest)†		Acetate Clearance (Dobutamine)‡		Mismatch		Match	
	r	p	r	p	r	p	r	p	r	p	r	p
LVEDP	0.09	0.71	−0.28	0.21	0.08	0.81	−0.08	0.79	−0.003	0.99	0.26	0.27
LVEF	−0.01	0.97	0.41	0.02	−0.03	0.93	0.06	0.85	−0.19	0.47	−0.11	0.66
DLVWS	0.07	0.77	−0.20	0.33	−0.07	0.86	0.22	0.57	0.14	0.62	0.18	0.58
SLVWS	−0.49	0.57	−0.61	0.01	−0.46	0.30	−0.82	0.03	0.64	0.02	0.21	0.43
$\dot{V}O_2$max	−0.15	0.58	0.42	0.04	−0.53	0.28	−0.28	0.60	0.49	0.15	−0.08	0.74

*Ratio of MBF during dipyridamole and MBF at rest. †Acetate clearance rate (k_{mono}) at rest. ‡Acetate clearance rate (k_{mono}) during low dose (20 μg/kg per min) dobutamine infusion.

DLVWS = diastolic left ventricular wall stress; LVEDP = left ventricular end-diastolic pressure (during left angiography); LVEF = left ventricular ejection fraction; match: see text for definition; mismatch: see text for definition; MBF = myocardial blood flow; SLVWS = systolic left ventricular wall stress; $\dot{V}O_2$max = peak oxygen consumption during exercise.

dipyridamole). Consequently, global MBF reserve was reduced in patients with IDC as compared with control subjects (1.72 ± 0.21 vs. 2.71 ± 0.10, p = 0.03). The impaired MBF reserve in patients with IDC showed a correlation with LVEF (r = 0.4, p = 0.02) and with $\dot{V}O_2$max (r = 0.4, p = 0.04) (Table 2) and was significantly lower in patients in NYHA functional class III than in those in class II (p = 0.004) (Fig. 3). Systolic wall stress showed a trend toward a negative correlation with MBF at rest (r = −0.49, p = 0.057) and a significant correlation with MBF during dipyridamole (r = −0.65, p = 0.007) (Table 2 and Fig. 4). For diastolic wall stress there were no such (significant) correlations (Table 2).

Glucose utilization (^{18}FDG studies). Total ^{18}FDG uptake in patients with IDC (50 ± 20 μmol/min per 100 g) was not different from that of healthy volunteers (60 ± 18 μmol/min per 100 g). However, when uptake of ^{18}FDG was related to perfusion (hyperemic ^{13}N-ammonia studies), mismatch was observed in 16 (76%) of the 22 patients with IDC, but in 0% of healthy control subjects (p = 0.003). In these 16 patients, 17.3 ± 8% of the myocardium showed this mismatch pattern (range 6% to 40%); the polar map showed clear confluent regions with mismatch. In 14 patients, 16.4 ± 9% of the myocardium showed a match pattern (range 5% to 28%). Further, in the patients with IDC, increased systolic wall stress was associated with extent of mismatch (r = 0.64, p = 0.02) (Table 2). For diastolic wall stress this correlation was not significant (r = 0.14, p = 0.62).

Myocardial oxidative metabolism (^{11}C-acetate studies). Dobutamine infusion had a similar effect on the rate–pressure product in patients with IDC and healthy volunteers (mean ratio 2.4 ± 0.4 and 2.2 ± 0.3, respectively, p = NS). In patients with IDC, ^{11}C-acetate clearance (k_{mono}) at rest (0.057 ± 0.014 min^{-1}) and after dobutamine (0.089 ± 0.021 min^{-1}) was not different from that of healthy control subjects (0.052 ± 0.012 and 0.101 ± 0.032 min^{-1}, respectively, p = NS). However, the ratio of ^{11}C-acetate clearance (k_{mono} dobutamine/k_{mono} rest) in patients with IDC was 1.6 ± 0.3 vs. 2.0 ± 0.2 in control subjects (p = 0.04). When global MBF reserve was related to global k_{mono} ratio (increase in oxygen consumption after dobutamine) there

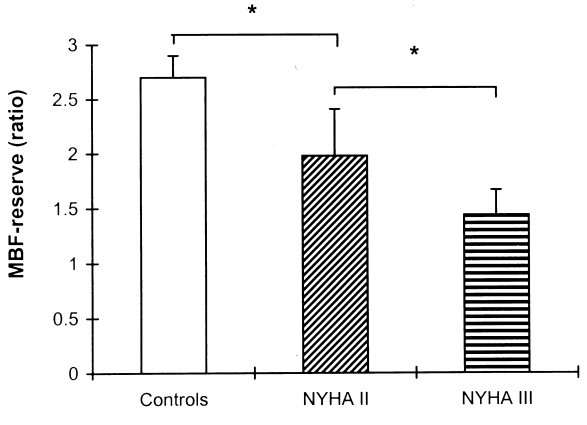

Figure 3. Global MBF reserve in control subjects and in patients in New York Heart Association (NYHA) functional classes II and III. *p < 0.05.

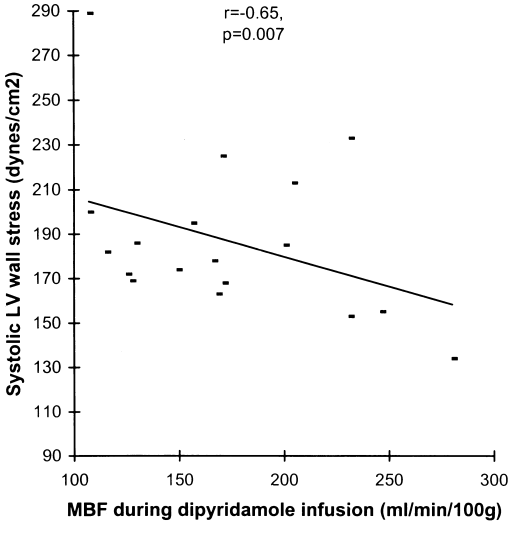

Figure 4. Correlation between global MBF during dipyridamole infusion and LV systolic wall stress in patients with IDC.

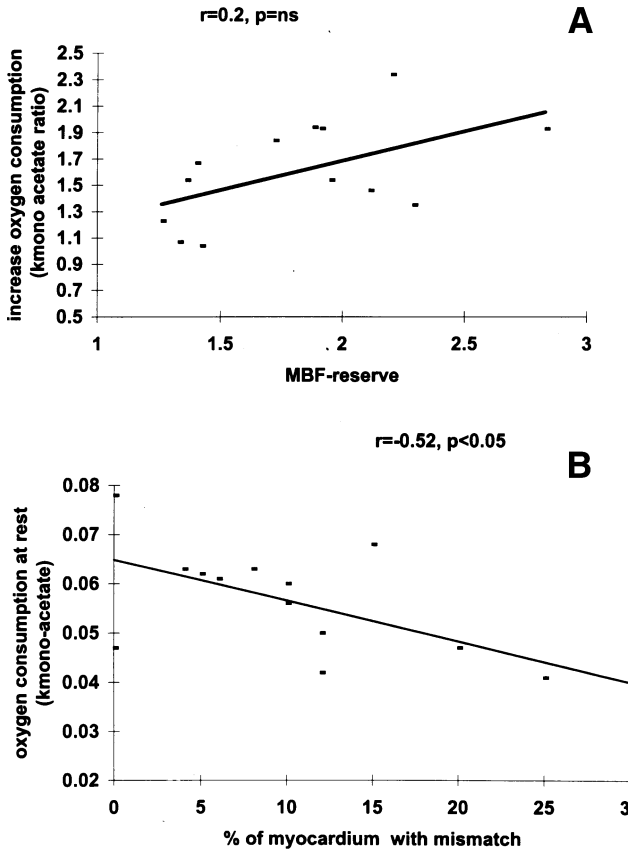

Figure 5. A, Correlation between global MBF reserve and ^{11}C-acetate clearance rate ratio (ratio of ^{11}C-acetate clearance rates during dobutamine infusion and clearance rates at rest). Note that low dose dobutamine infusion did not exhaust the dipyridamole-determined MBF reserve. **B,** Correlation between global ^{11}C-acetate clearance rate (k_{mono} = oxygen consumption) at rest and percent myocardium showing mismatch.

was a nonsignificant relation ($r = 0.2$, $p = 0.2$) (Fig. 5A). There was a significant negative relation between global ^{11}C-acetate clearance rates and percent myocardium with mismatch ($r = -0.52$, $p < 0.05$) (Fig. 5B). Global systolic wall stress correlated negatively with global k_{mono} during submaximal dobutamine infusion ($r = -0.82$, $p = 0.025$) and positively with percent myocardium with match ($r = 0.61$, $p = 0.02$).

Regional measurements. Table 3 shows measurements in normal regions, mismatch regions and match regions. Rest MBF was not different between the three regions. However, during the dipyridamole stress test, an increase in MBF was higher in the normal regions, leading to a higher MBF reserve (1.90 ± 0.18 in normal regions; 1.58 ± 0.13 in mismatch; 1.53 ± 0.10 in match). The FDG uptake was highest in the mismatch regions (64 ± 14 μmol/min per 100 g) and lowest in the match regions (43 ± 12 μmol/min per 100 g). In normal regions, FDG uptake was 56 ± 12 μmol/min per 100 g. At rest, k_{mono} (oxygen consumption) was not different in the three regions. During dobutamine, the increase in oxygen consumption was significantly higher in the mismatch regions than in the normal regions (ratio 1.73 ± 0.22 vs. 1.53 ± 0.22, respectively). The FDG uptake and oxygen consumption (k_{mono}) showed a significant negative correlation ($r = -0.65$, $p < 0.05$) in the mismatch regions, but not in other regions.

DISCUSSION

Main findings. The present study shows normal myocardial perfusion at rest but impaired MBF reserve in patients with IDC, thereby confirming previous findings (18). Furthermore, it reveals that MBF reserve impairment was related to severity of heart failure and to systolic LV wall stress. In addition, in the majority of patients with IDC (76%), mismatch (perfusion/metabolism) was observed in a substantial part of the myocardium, and in 64% of the patients match was observed. Furthermore, although rest global and regional oxygen consumptions were normal, a negative correlation between rest oxygen consumption and extent of mismatch was found, indicating regional adaption to lowered metabolic needs at rest. In addition, oxidative metabolism during submaximal adrenergic drive appeared disturbed (i.e., oxygen consumption shows a more rapid increase in mismatch regions as compared with normal regions). Finally, in mismatch regions ^{18}FDG uptake showed a negative correlation with k_{mono} at rest, suggesting a switch from aerobic (^{11}C-acetate clearance rate) to anaerobic metabolism (glucose uptake). Furthermore, high systolic wall stress was associated with reduced oxygen consumption during stress and with the extent of match and mismatch. These findings support the notion of a mainly stress-induced imbalance between oxygen demand (oxygen utilization) and supply, leading to regional metabolic changes compatible with hibernation or chronic ischemia.

Decreased global flow reserve in patients with IDC. The regulation of MBF in patients with cardiac disease is a complex phenomenon. It depends on coronary perfusion pressure, lumen integrity and vasomotor control in epicardial conduit vessels, function of the coronary microcirculation as well as extravascular forces related to intramyocardial pressure or wall stress (20,21). In the present study, the impairment of global MBF reserve was related to the degree of LV dysfunction, NYHA functional class and LV systolic wall stress. Under physiologic conditions an increase in LV wall stress is associated with increased MBF and higher oxygen consumption. However, under pathophysiologic conditions, such as LV hypertrophy and cardiomyopathy, the reverse may occur, potentially setting the stage for myocardial ischemia. Vatner et al. (21) demonstrated in dogs with LV hypertrophy and LV failure that that blood flow reserve was impaired by elevated LV systolic wall stress (most obvious in the subendocardium), which was paralleled by myocardial ischemia, as evidenced by decreased contractility. At a later point in time myocardial fibrosis was observed in the subendocardium. In the present study, the

JACC Vol. 35, No. 1, 2000
January 2000:19–28

Table 3. Positron Emission Tomographic Measurements in the Three Different Regions

	Mismatch Regions	Match Regions	Normal Regions
Percent myocardium	17.3 ± 8%	16.4 ± 9%	
No. of patients	16	14	
Rest MBF (ml/min per 100 g)	102 ± 13	100 ± 10	115 ± 18
Dipyridamole MBF (ml/min per 100 g)	156 ± 26	146 ± 23	219 ± 34*
MBF reserve (ratio)	1.58 ± 0.13	1.53 ± 0.10	1.90 ± 0.18*
^{18}FDG uptake (μmol/min per 100 g)	64 ± 14*	43 ± 12*	56 ± 12*
Rest k_{mono} (min^{-1})	0.060 ± 0.011	0.056 ± 0.009	0.057 ± 0.010
Dobutamine k_{mono} (min^{-1})	0.104 ± 0.017*	0.084 ± 0.018	0.087 ± 0.016
k_{mono} ratio	1.73 ± 0.22*	1.50 ± 0.21	1.53 ± 0.22
Correlation between MBF and k_{mono} (rest)	0.5 (p = NS)	0.6 (p < 0.05)	0.9 (p < 0.05)
Correlation between ^{18}FDG and k_{mono} (rest)	−0.65 (p < 0.05)	−0.25 (p = NS)	−0.30 (p = NS)

*p < 0.05 vs. other two groups. Data are presented as the mean value ± SD.
^{18}FDG (fluorine-18 deoxyglucose) uptake = glucose metabolism; k_{mono} (^{11}C-acetate clearance) = estimate of oxygen consumption; k_{mono} ratio = factor indicating an increase of oxygen consumption during low dose (20 μg/kg per min) dobutamine infusion; correlation coefficient of MBF and k_{mono} (rest) indicates the degree to which MBF determines oxygen consumption (see text); the correlation of ^{18}FDG and k_{mono} (rest) indicates the degree to which aerobic and anaerobic metabolism are linked (see text); MBF = myocardial blood flow.

match regions might represent such regions with myocardial fibrosis—the clinical counterpart being myocardial fibrosis found in endomyocardial biopsies. Intrinsic functional vascular wall abnormalities (e.g., endothelial dysfunction) may also lead to impairment of MBF reserve and ischemia in CHF (3,22,23). In addition, it may relate to high levels of circulating vasoconstrictor neurohormones like norepinephrine, angiotensin II and endothelin. In addition, long-term elevations of these neurohormones may induce structural vascular changes that may potentially impair endothelium-induced vasodilation of the coronary vasculature, as observed in patients with hypertension (24).

Global glucose (^{18}FDG) and oxidative (^{11}C-acetate) metabolism. Global data showed match and mismatch defects concerning FDG uptake and MBF reserve in 76% of patients with IDC but not in normal control subjects. In general, mismatch is considered to represent a kind of metabolic derangement if not ischemia. Mismatch and match appeared to be confined to confluent myocardial regions. Global rest and stress-induced oxygen consumptions seem normal but their ratio was significantly lower in patients with IDC than in control subjects. This indicates that on a global basis the increment in oxygen consumption during adrenergic stress is less marked. Further analysis within the group of patients with IDC revealed that this was not necessarily due to the reduced MBF reserve seen in our patients with IDC. Instead, decreased adrenergic-dependent oxygen consumption seemed to be associated with high systolic wall stress, and, in turn, high wall stress was paralleled by a larger amount of myocardium with mismatch. Our interpretation of these findings is that in the course of the disease, high wall stress may provoke ischemic conditions by limiting peak blood flow and increasing oxygen demand, which in turn leads to hibernation and hence decreased oxygen consumption during stress. In this respect, it is interesting to note the inverse association between systolic wall stress and global MBF reserve. Considering this, provocation of ischemia by high wall stress may appear an important supervening mechanism causing deterioration of LV function in patients with IDC, but this notion needs further study.

Regional measurements. In the areas with "ischemic" metabolic changes (i.e., mismatch areas) the flow reserve is most impaired, whereas ^{18}FDG uptake is increased in these regions. The rest oxygen consumption (k_{mono}) was similar among regions that had been shown previously and may be ascribed to a relatively high increase in oxygen extraction in the abnormal areas (25). However, quite unexpectedly, dobutamine stimulation provoked a significantly higher (rather than lower) oxygen consumption in the mismatch regions as compared with the match and normal regions. Dobutamine (dose of 20 μg/kg per min) did not exhaust global flow reserve (defined as dipyridamole/rest flow), indicating that adrenergic stimulation was submaximal. The ^{11}C-acetate findings suggest that during submaximal adrenergic stimulation, oxygen consumption increases faster than it does in normal regions, suggesting higher oxygen demand in the mismatch regions during similar stimulation. The regionally high oxygen consumption after submaximal adrenergic stimulation may be due to a relative increase in (ischemia-induced) beta-adrenoceptor density in the mismatch regions (26) or to an increased regional LV wall stress (27). The latter may represent higher extravascular flow impedance and higher oxygen demand. Our ^{11}C-acetate data suggest that the wall motion response to submaximal dobutamine (20 μg/kg per min) is unaffected or even increased in the mismatch areas, rather than decreased. This is supported by the findings of Cohen et al. (28), who found in patients with IDC (age 57 ± 12 years, LVEF 0.27 ± 0.09) that the inotropic response to 40 μg/kg per min was unchanged or increased in 21 of 22 patients. Whether all this leads to ischemia is questionable. However, high dose

dobutamine may provoke ischemia by exhausting flow reserve, while potentially further increasing oxygen demand. The concept of ischemia in IDC is further supported by the presumed switch from aerobic to anaerobic metabolism in the mismatch areas. With this concept one must assume that ischemia is not continuously present but develops only during intermittent high grade adrenergic stimulation leading to repetitive stunning and hibernation (29).

Study limitations. To keep the physiologic conditions constant, we did not use the technique of hyperinsulinemic, euglycemic clamping. With the method we employed, the glucose uptake was probably limited by decreased insulin sensitivity, as is often the case in CHF (30). By using the clamping technique, glucose uptake would probably have been higher, and thus it is possible that we underestimated the extent of mismatch in the present study. Noninvasive detection and quantitation of myocardial ischemia remains difficult (31), but both ^{18}FDG and ^{11}C-acetate studies using PET provide supportive data for ischemia as a mechanism. The combination of decreased MBF reserve and increased ^{18}FDG uptake (i.e., "mismatch" pattern) is considered to indicate myocardial ischemia (9). Although this notion is usually employed in patients with coronary artery disease to assess viability (32), it was also used in the present study of patients with IDC. In support of the use of the mismatch notion in patients with IDC, we want to draw attention to the fact that mismatch was not only the consequence of reduced flow reserve but also significantly increased ^{18}FDG uptake. The question remains as to what triggers the regional mismatch (i.e., local "ischemic" changes in patients with IDC) and why certain regions are affected and others unaffected. Furthermore, the present data cannot define the clinical role of local ischemia in IDC. However, it is tempting to assume that ischemia provokes progressive deterioration of ventricular function. How far the mismatch areas may normalize again in terms of flow, metabolism and oxygen consumption, or deteriorate into match (i.e., fibrotic) areas, is another important question that deserves further study. The present study did not evaluate regional differences in rest wall motion, and therefore the functional consequences of the hypothesized ischemia cannot be addressed. Mitral regurgitation would be important for evaluating the described flows and oxidative metabolism rates and also might be relevant for stress calculations. Although we do not have individual quantitative data of mitral regurgitation in these patients, mitral regurgitation worse than grade II was not found in our patients.

Clinical implications. It has always been assumed that myocardial ischemia does not play a role in IDC. However, if myocardial ischemia is indeed present in patients with IDC, it has important implications for the pathophysiology of the disease, and it may modify drug treatment. In this respect, it is tempting to speculate that the favorable effects in studies with beta-blockers (Cardiac Insufficiency Bisoprolol Study [CIBIS-1]) and also with the calcium channel blocker amlodipine (Prospective Randomized Amlodipine Survival Evaluation [PRAISE]) in patients with CHF and IDC, may be partly due to their anti-ischemic effects (33,34). In these studies more pronounced effects were observed in patients with IDC than in those with CHF due to coronary artery disease. A potential explanation for these somewhat unexpected findings is the fact that patients with CHF and IDC are basically not tested with anti-anginal drugs, and the effects of anti-ischemic drugs may therefore be more pronounced.

Acknowledgment

We thank P. J. de Kam, from the Statistical Department of the Trial Coordination Centre, University Hospital, Groningen, The Netherlands, for his statistical advice.

Reprint requests and correspondence: Dr. D. J. van Veldhuisen, Department of Cardiology/Thoraxcenter, University Hospital Groningen, P.O. Box 30.001, 9700 RB Groningen, The Netherlands. E-mail: d.j.van.veldhuisen@thorax.azg.nl.

REFERENCES

1. Dec WG, Fuster V. Idiopathic dilated cardiomyopathy. N Engl J Med 1994;331:1564–75.
2. Michels VV. Progress in defining the causes of idiopathic dilated cardiomyopathy. N Engl J Med 1993;329:960–1.
3. Treasure CB, Vita JA, Cox DA, et al. Endothelium-dependent dilation of the coronary microvasculature is impaired in dilated cardiomyopathy. Circulation 1990;83:772–9.
4. Juillière Y, Marie PY, Danchin N, et al. Radionuclide assessment of regional differences in left ventricular wall motion and myocardial perfusion in idiopathic dilated cardiomyopathy. Eur Heart J 1993;14: 1163–9.
5. Phelps ME, Mazziotta JC, Schelbert HR, editors. Positron Emission Tomography and Autoradiography: Principles and Applications for the Brain and the Heart. New York: Raven Press, 1986.
6. Schelbert HR, Phelps ME, Huang SC, et al. N-13 ammonia as an indicator of myocardial blood flow. Circulation 1981;63:1259–72.
7. Bellina CR, Parodi O, Camici P, et al. Simultaneous in vitro and in vivo validation of nitrogen-13-ammonia for the assessment of regional myocardial blood flow. J Nucl Med 1990;31:1335–43.
8. Dilsizian V, Bonow RO. Current diagnostic techniques of assessing myocardial viability in patients with hibernating and stunned myocardium. Circulation 1993;87:1–20.
9. Tamaki N, Yonekura Y, Yamashita K, et al. Positron-emission tomography using fluorine-18 deoxyglucose in evaluation of coronary artery bypass grafting. Am J Cardiol 1989;64:860–5.
10. Armbrecht JJ, Buxton DB, Schelbert HR. Validation of [1-^{11}C] acetate as a tracer for noninvasive assessment of oxidative metabolism with positron emission tomography in normal, ischemic, postischemic, and hyperemic canine myocardium. Circulation 1990;81:1594–605.
11. Beanlands RS, Bach DS, Raylman R, et al. Acute effects of dobutamine on myocardial oxygen consumption and cardiac efficiency measured using carbon-11 acetate kinetics in patients with dilated cardiomyopathy. J Am Coll Cardiol 1993;22:1389–98.
12. van den Broek SAJ, van Veldhuisen DJ, de Graeff PA, Landsman ML, Hillege H, Lie KI. Comparison between New York Heart Association classification and peak oxygen consumption in the assessment of functional status and prognosis in patients with mild to moderate chronic congestive heart failure secondary to either ischemia or idiopathic dilated cardiomyopathy. Am J Cardiol 1992;70:359–63.
13. Blanksma PK, Willemsen ATM, Meeder JG, et al. Quantitative myocardial mapping of perfusion and metabolism using parametric polar map displays in cardiac PET. J Nucl Med 1995;36:153–8.
14. Choi Y, Hawkins RA, Huang SC, et al. Parametric images of glucose

generated from dynamic cardiac PET and 2-[^{18}F]fluoro-2-deoxy-D-glucose studies. J Nucl Med 1991;32:733–8.
15. Porenta G, Kuhle W, Czernin J, et al. Semiquantitative assessment of myocardial blood flow and viability using polar map display of cardiac PET images. J Nucl Med 1992;33:1628–36.
16. Shah A, Schelbert HR, Schwaiger M, et al. Measurement of regional myocardial blood flow with N-13 ammonia and positron emission tomography in intact dogs. J Am Coll Cardiol 1985;5:92–100.
17. Patlak CS, Blasberg RG. Graphical evaluation of blood-to-brain transfer constants from multiple-time uptake data: generalizations. J Cereb Blood Flow Metab 1985;5:584–90.
18. Vanoverschelde JJ, Wijns W, Depré C, et al. Mechanisms of chronic regional postischemic dysfunction in humans: new insights from the study of noninfarcted collateral-dependent myocardium. Circulation 1993;87:1513–23.
19. Reichek N, Wilson J, St. John Sutton MJ, Plappert TA, Goldberg S, Hirschfeld JW. Noninvasive determination of left ventricular end-systolic stress: validation of the method and initial application. Circulation 1982;65:99–108.
20. Maseri A, Crea F, Cianflone D. Myocardial ischemia caused by distal coronary vasoconstriction. Am J Cardiol 1992;70:1602–5.
21. Vatner SF, Hittinger L. Coronary vascular mechanisms involved in decompensation from hypertrophy to heart failure. J Am Coll Cardiol 1993;22:34A–40A.
22. Drexler H, Hayoz D, Munzel T, et al. Endothelial function in chronic heart failure. Am J Cardiol 1992;69:1596–601.
23. Neglia D, Parodi O, Gallopin M, et al. Myocardial blood flow response to pacing tachycardia and to dipyridamole infusion in patients with dilated cardiomyopathy without overt heart failure: a quantitative assessment by positron emission tomography. Circulation 1995;92: 796–804.
24. Clozel M. Mechanism of action of angiotensin converting enzyme inhibitors on endothelial function in hypertension. Hypertension 1991;18 Suppl 4:1137–42.
25. Czernin J, Porenta G, Brunken R, et al. Regional blood flow, oxidative metabolism, and glucose utilization in patients with recent myocardial infarction. Circulation 1993;88:884–95.
26. Ungerer M, Kessebohm K, Kronsbein K, Lohse MJ, Richardt G. Activation of beta-adrenergic receptor kinase during myocardial ischemia. Circ Res 1996;79:455–60.
27. Bach DS, Beanlands RS, Schwaiger M, Armstrong WF. Heterogeneity of ventricular function and myocardial oxidative metabolism in nonischemic dilated cardiomyopathy. J Am Coll Cardiol 1995;25: 1258–62.
28. Cohen A, Chauvel C, Benhalima B, Guyon P, Desert I, Valty J. Is dobutamine stress echocardiography useful for noninvasive differentiation of ischemic from idiopathic dilated cardiomyopathy? Angiology 1997;48:783–93.
29. Sawada S, Eisner G, Segar DS, et al. Evaluation of patterns of perfusion and metabolism in dobutamine-responsive myocardium. J Am Coll Cardiol. 1997;29:55–61.
30. Marinho NVS, Keogh BE, Costa DC, Lammertsma AA, Ell PJ, Camici PG. Pathophysiology of chronic left ventricular dysfunction: new insights from the measurement of absolute myocardial blood flow and glucose utilization. Circulation 1996;93:737–44.
31. Cannon RO III. Does coronary endothelial dysfunction cause myocardial ischemia in the absence of obstructive coronary artery disease (editorial)? Circulation 1997;96:3390–5.
32. Mäki M, Luotolahti M, Nuutila P, et al. Glucose uptake in the chronically dysfunctional but viable myocardium. Circulation 1996;93: 1658–66.
33. CIBIS Investigators and Committees. The Cardiac Insufficiency Bisoprolol Study (CIBIS): a randomized trial of beta-blockade in heart failure. Circulation 1996;90:1765–73.
34. Packer M, O'Connor CM, Ghali JK, et al., for the Prospective Randomized Amlodipine Survival Evaluation Study Group. Effects of amlodipine on morbidity and mortality in severe chronic heart failure. N Engl J Med 1996;335:1107–14.